

Finding the stable mechanism of ring solitons in two-dimensional Fermi superfluids

Hao-Xuan Sun¹, Liu-Yang Cheng², Shi-Guo Peng² ^{*} Yan-Qiang Li¹ [†] and Peng Zou¹ [‡]

¹Centre for Theoretical and Computational Physics,

College of Physics, Qingdao University, Qingdao 266071, China and

²State Key Laboratory of Magnetic Resonance and Atomic and Molecular Physics,

Innovation Academy for Precision Measurement Science and Technology,

Chinese Academy of Sciences, Wuhan 430071, China

We theoretically investigate the stable mechanism of a ring soliton in two-dimensional Fermi superfluids by solving the Bogoliubov-de Gennes equations and their time-dependent counterparts. In the uniform situation, we discover that the ring soliton is always driven away from its initial location, and moves towards the edge due to a curvature-induced effective potential. The ring soliton is impossible to remain static at any location in the uniform system. To balance the density difference between the ring soliton's two sides, a harmonic trap is introduced, which can exert an effect to counterbalances the curvature-induced effective potential. This enables the ring dark soliton to become a stable state at a particular equilibrium position r_s , where the free energy of the ring dark soliton just reaches the maximum value. Once ring soliton is slightly deviated from r_s , some stable periodic oscillations of ring soliton around r_s will turn out. Some dissipation will possibly occur to ring soliton once its minimum radius is comparable to the healing length of soliton's Friedel oscillation. This dissipation will increase the oscillation amplitude and finally make the ring soliton decay into sound ripples. Our research lays the groundwork for a more in-depth understanding of the stable mechanism of a ring dark soliton in the future.

I. INTRODUCTION

As a spatially localized wave, the soliton originates from the interplay between dispersion and non-linearity of the underlying system [1]. Usually, the dark soliton is a kind of low-energy solution of many-body systems, and exerts a crucial influence on the dynamical behaviors of the system. In the past three decades, much research attention has focused on solitons of atomic Bose-Einstein condensates (BECs) [2]. Many members of the soliton family are investigated in different physical systems (or matter states), including bright solitons in attractive BECs and dark solitons in repulsively interacting BECs [3–7]. Similar research has also been carried out in Fermi superfluids, to study the static dark soliton and the dynamical motion behavior of solitons [13–15]. The decay mechanism of solitons, known as snake instability, has also been theoretically investigated [17]. Since the realization of spin-orbit-coupling (SOC) effect in ultracold atomic gases, a novel Majorana soliton and its distinct motion mechanism have been discovered in SOC Fermi superfluids [20–23]. The soliton can be generated by a phase-imprinting technique [18, 19]. Moreover, it has been experimentally fabricated to observe its dynamical behavior [9].

A typical characteristic of a dark soliton is that there is a phase jump $\delta\phi = \pi$ exhibited by the phase of the order parameter across the two sides of the soliton's position. The typical soliton discussed above is a linear one, in which the value of the phase jump $\delta\phi$ changes along

an ideal straight line. This also marks the location of the soliton, where the core density is usually lower than the bulk density of the system. Also the soliton displays some fluctuations in both density and order parameter within the regime of healing length, which is called Friedel oscillation [13]. If certain perturbations disrupt the straight-line geometry of linear solitons, the snake instability will cause the soliton to bend and possibly decay into sound waves, or vortices, etc [17]. Generally, it seems that all the bending or disturbing behavior in the perpendicular direction of the soliton will break its stability. However, this is not always true. Besides the linear soliton, it is of great interest to explore the existence of other geometries of stable solitons. In fact, ring solitons have been also investigated in BECs. The geometric locus of its phase jump forms an ideal circular shape [8, 10]. However, this ring soliton is usually not a stable state. It often tends to exhibit some extraordinary dynamical behaviors and evolves into various forms such as multiple concentric ring solitons, vortex-antivortex pairs, or a complex pattern structure [8, 11, 24, 25]. It is interesting to understand and control these rich dynamical behaviors, which is usually not easy to carry out. In Fermi superfluid, there are quite a few discussions about the ring soliton currently. Reference [12] introduces stable ring solitons in an imbalanced fermionic system with a phenomenological Ginzburg-Landau theory. In this paper, we will study the ring soliton in balanced two-dimensional (2D) Fermi superfluids with more exact static and time-dependent Bogoliubov-de Gennes (BdG) equations. The purpose of this paper is to better understand the motion and decay mechanism of ring solitons and find the possible physical explanation behind them.

This paper is organized as follows. In the subsequent section, we will firstly introduce the static BdG equations

^{*} pengshigu@wipm.ac.cn

[†] lyq_qdsd@163.com

[‡] phy.zoupeng@gmail.com

and their time-dependent counterparts, by which to examine the stability of ring solitons. In Sec. III, we use four subsections to investigate the dynamical behavior of ring solitons in both uniform and trapped systems, to analyze the stability and decay behavior of ring solitons. Finally, our conclusions are given in Sec. IV.

II. METHODS

We consider a 2D Fermi superfluid with balanced populations of the two spin components at zero temperature. Particles of different spin will experience a s-wave contact interaction. Within the mean-field theory, the many-body Schrödinger equations of this system can be well reduced to BdG equations

$$\begin{bmatrix} \hat{H}_S & \Delta(\mathbf{r}) \\ \Delta^*(\mathbf{r}) & -\hat{H}_S \end{bmatrix} \begin{bmatrix} u_\eta(\mathbf{r}) \\ v_\eta(\mathbf{r}) \end{bmatrix} = E_\eta \begin{bmatrix} u_\eta(\mathbf{r}) \\ v_\eta(\mathbf{r}) \end{bmatrix}, \quad (1)$$

where $\hat{H}_S = -\nabla^2/2m + V(\mathbf{r}) - \mu$ is the single particle Hamiltonian in an external potential $V(\mathbf{r})$ with mass m and chemical potential μ . E_η is the quasiparticle eigenenergy with the corresponding quasiparticle wave functions u_η and v_η , which are normalized by $\int d\mathbf{r}[v_\eta(\mathbf{r})v_{\eta'}^*(\mathbf{r}) + u_\eta(\mathbf{r})u_{\eta'}^*(\mathbf{r})] = \delta_{\eta\eta'}$. Here and hereinafter, we set the Planck constant $\hbar = 1$. These BdG equations should be self-consistently solved with the order parameter (or gap) function

$$\Delta(\mathbf{r}) = g \sum_\eta u_\eta(\mathbf{r})v_\eta^*(\mathbf{r}) \quad (2)$$

and total density function

$$n(\mathbf{r}) = 2 \sum_\eta |v_\eta(\mathbf{r})|^2. \quad (3)$$

Here g is the bare interatomic interaction strength, and it should be regularized by

$$\frac{1}{g} = - \sum_k \left(\frac{1}{E_b + 2\epsilon_k} \right), \quad (4)$$

in which $\epsilon_k = k^2/2m$ and binding energy E_b describes the strength of interaction. A cutoff energy E_c is considered during the summation of possible energy levels in the numerical calculation, namely $0 < E_\eta < E_c$. To investigate the dynamics of the system, time-dependent BdG equations, whose expressions are

$$\begin{bmatrix} \hat{H}_S & \Delta(\mathbf{r}, t) \\ \Delta^*(\mathbf{r}, t) & -\hat{H}_S \end{bmatrix} \begin{bmatrix} u_\eta(\mathbf{r}, t) \\ v_\eta(\mathbf{r}, t) \end{bmatrix} = i \frac{\partial}{\partial t} \begin{bmatrix} u_\eta(\mathbf{r}, t) \\ v_\eta(\mathbf{r}, t) \end{bmatrix}, \quad (5)$$

are utilized to observe the time evolution of any initial state. The free energy of the system is

$$F = \int d\mathbf{r} \sum_\eta [2(\mu - E_\eta) |v_\eta|^2 + \Delta^* u_\eta v_\eta^*] + \mu N, \quad (6)$$

where $N = \int d\mathbf{r} n(\mathbf{r})$ is the total particle number of the system. In the following, we will consider both the uniform system ($V(\mathbf{r}) = 0$) and the trapped one ($V(\mathbf{r}) \neq 0$). These two cases have their own typical wave vector k_F and typical energy $E_F = k_F^2/2m$, which are used to do dimensionless treatment of all related physical quantities in the following discussion.

Owing to the geometric symmetry of the ring soliton, we study the system with a 2D circular hard-wall environment with a maximum radius R . Naturally, it is better to introduce the position parameter $\mathbf{r} = (r, \theta)$ in the polar coordinates instead of $\mathbf{r} = (x, y)$ in Cartesian coordinates. In this case, the quasiparticle wave functions u_η and v_η could be expanded with a set of normalized basis functions $\psi_{jl}(r) = \sqrt{2}J_l(r\alpha_{jl}/R)/RJ_{l+1}(\alpha_{jl})$, where α_{jl} is the j th zero of the Bessel function $J_l(r)$. Namely $u_\eta(r, \theta) = \sum_j c_{\eta j} \psi_{jl}(r)e^{il\theta}/\sqrt{2\pi}$ and $v_\eta(r, \theta) = \sum_j d_{\eta j} \psi_{jl}(r)e^{il\theta}/\sqrt{2\pi}$. Then solving BdG Eqs. 1 is reduced to a mathematical matrix diagonalization problem with

$$\begin{bmatrix} H_{jj'}^l & \Delta_{jj'}^l \\ \Delta_{j'j*}^l & -H_{jj'}^l \end{bmatrix} \begin{bmatrix} c_{\eta j} \\ d_{\eta j} \end{bmatrix} = E_\eta \begin{bmatrix} c_{\eta j} \\ d_{\eta j} \end{bmatrix}, \quad (7)$$

in which $H_{jj'}^l = (a_{jl}^2/R^2 - \mu)\delta_{jj'} + V_{jj'}^l$ and $\Delta_{jj'}^l = \int \phi_{jl}(r)\Delta(r)\phi_{j'l}^*(r)rdr$. In our numerical calculation, we have set parameters $E_c = 25E_F$ with the maximum angular quantum number $|l|_{max} = 130$ and the zero-point number $j_{max} = 60$, whose values we have checked are large enough to carry out numerical calculations.

III. RESULTS OF THE RING SOLITON

A. Uniform system

The uniform system has a well-defined bulk density n_0 , by which the typical wave vector $k_F = \sqrt{2\pi n_0}$. Generally all possible many-body solutions of a fermionic system can be derived by self-consistently solving the Bogoliubov-de Gennes (BdG) equations shown in Eq. 1, the order parameter equation presented in Eq. 2, and the density equation given in Eq. 3. In this numerical process, it is necessary to iterate over all possible degrees of freedom to achieve a stable state. For example, one needs to iterate both the chemical potential μ and the spatial distribution of the order parameter $\Delta(\mathbf{r})$ in order to get a stable linear dark soliton in the uniform system. In the case of the ring soliton, its radius plays the role of another new degree of freedom. However, there is no means for us to obtain an equation for the exact radius. To overcome this question, our strategy is to consider temporarily the ring soliton in a uniform system by iterating solely the chemical potential μ and order parameter distribution $\Delta(\mathbf{r})$ to obtain an instantaneous zero-velocity state. Subsequently, a time-dependent simulation of this instantaneous state is conducted to verify its stability.

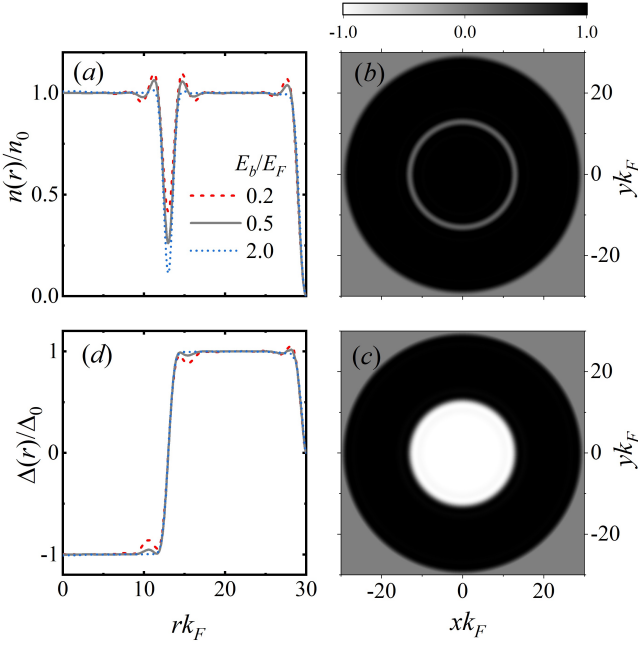


Figure 1. The density (upper panels) and order parameter (lower panels) distributions of an instantaneous ring dark soliton in both the radial direction (left panels) and x - y plane (right panels). The soliton is located at $r_0 k_F = 13.0$. The binding energy $E_b = 0.5E_F$.

Similar to the case of obtaining a linear dark soliton, we firstly guess an initial radius distribution of the order parameter $\Delta(r)$ with a phase jump $\delta\phi = \pi$ at a certain location r_0 , whose value is far from the center and the edge to avoid the influence of them. By solving self-consistently Eqs. 1, 2 and 3, we obtain an instantaneous zero-velocity solution of the ring dark soliton at $r_0 k_F = 13.0$. As depicted in Fig. 1, the upper two panels illustrate the spatial distribution of density, while the lower two panels exhibit the spatial distribution of the order parameter. The results of ring solitons in different binding energy E_b are also displayed in the left two panels. As the interaction strength E_b becomes increasingly larger, the location of the ring dark soliton presents a weaker and weaker Friedel oscillation in both density (panel (a)) and order parameter (panel (d)). Also, the ring dark soliton takes on a deeper and deeper density valley, shown by different line styles in panel (a), which makes soliton can be understood as a negative-mass wave.

To check the stability of the ring dark soliton, a time-dependent simulation is the most convenient way. A stable solution should exhibit a result that does not change with time. We utilize the above instantaneous state as an input one at time $t = 0$, and then evolve it by time-dependent BdG Eqs. 5. In some sense, this time-dependent approach plays the role of iterating the location of the ring dark soliton. The results are shown in Fig. 2. We obtain time evolutions of three ring dark solitons, which are initially located respectively at (a)

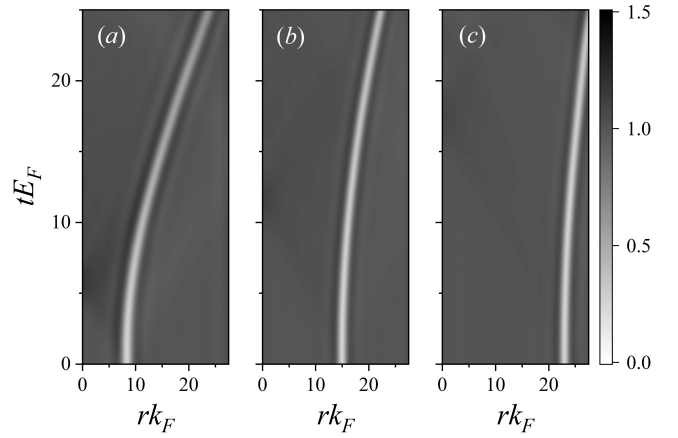


Figure 2. The time evolution of ring solitons in a uniform system with different initial locations, namely (a) $r_0 k_F = 7$, (b) $r_0 k_F = 15$ and (c) $r_0 k_F = 23$. The binding energy $E_b = 0.5E_F$.

$r_0 k_F = 7$, (b) $r_0 k_F = 15$ and (c) $r_0 k_F = 23$. Unfortunately, instead of fixing at their initial position r_0 all the time, all three panels demonstrate that ring solitons are driven away from r_0 , and move consistently outward to the edge induced by one common motion mechanism. This verifies that the ring solitons in the uniform system are not stable states. Also it can be readily observable that the nearer the initial location r_0 of a ring dark soliton is to the center, the farther it moves away from the center. It should be emphasized that there is no external trap in the uniform system to generate such an oriented motion.

Physically this common mechanism comes from the interplay between particles, whose strength should be also related to the geometric shape of ring solitons. The ring soliton is a kind of density-valley structure, and has fewer particles than the one in bulk position. The circular geometry of a ring soliton means that there will be more particles on the outer side than that inside. This kind of density distribution makes soliton a negative-mass density wave. At the same interaction strength between particles, more particles mean that the outside of ring soliton will possibly bring relatively more particles than that on the inner side, and induces the valley structure moving outwards. In the following, we will call this effect a curvature-induced effective potential, whose analytical expression is temporarily unknown and is absent in the conventional linear soliton due to its symmetric structure. The existence of the very curvature-induced effective potential not only explains the phenomenon in Fig. 2, but also makes it impossible for a ring dark soliton to become a stable state in the uniform system. In fact, the above discussions also shine a light on building a stable ring dark soliton in the non-uniform system.

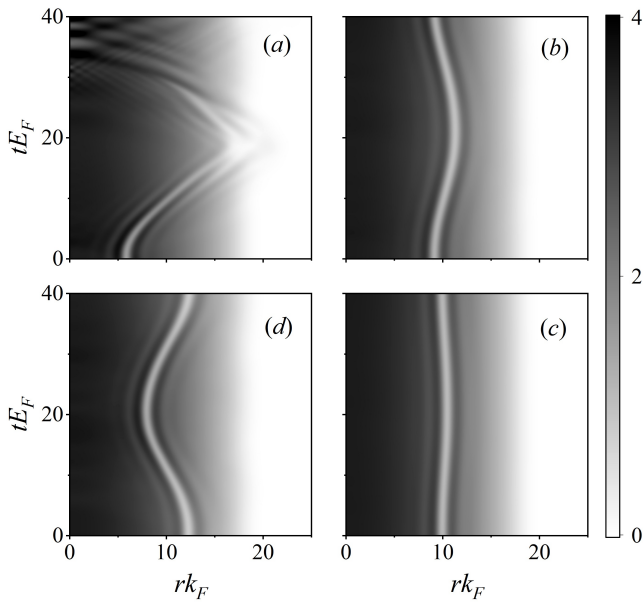


Figure 3. The time evolution of ring solitons in a harmonic trap with different initial locations, namely (a) $r_0 k_F = 5.5$, (b) $r_0 k_F = 9.0$, (c) $r_0 k_F = 10.1$ and (d) $r_0 k_F = 12.2$. The binding energy $E_b = 0.5E_F$.

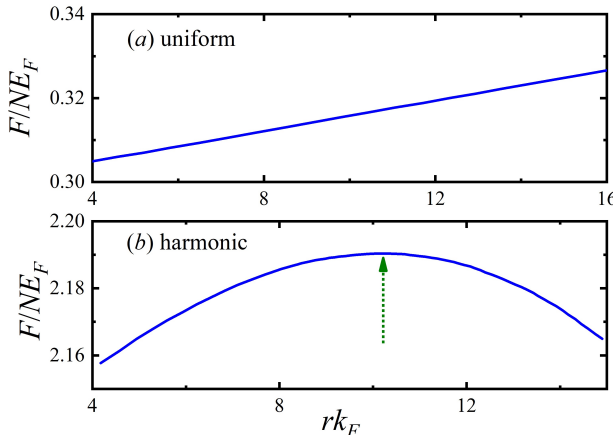


Figure 4. The free energy of instantaneous ring dark solitons at different locations. (a) uniform system with the same parameters as that in Fig. 1 and Fig. 2; (b) system in harmonic trap with the same parameters as that in Fig. 3.

B. System in a harmonic trap

By reducing the outer density of ring solitons while increasing their inner density, it is possible to counteract their tendency of moving outward. An intuitive strategy to generate this effect involves employing a harmonic trap $V(\mathbf{r}) = m\omega^2 r^2/2$, which is frequently utilized in experiments. Of course, the harmonic trap is not the only candidate external potential. In this part, we will consider the influence of a harmonic trap on the system and set the particle number N of the system as a constant value.

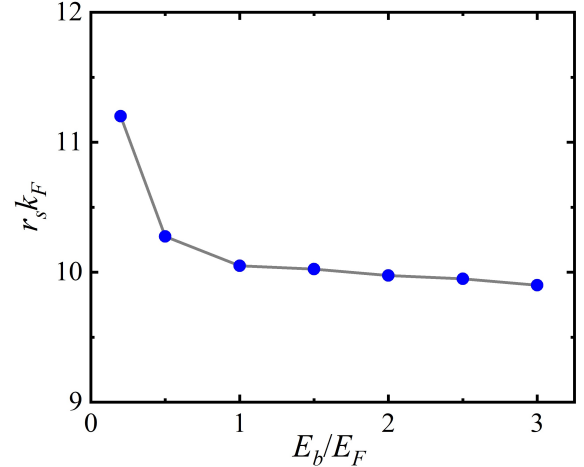


Figure 5. The stable location of a ring dark soliton in the harmonic trap system at different binding energy E_b .

In this case, the typical wave vector is $k_F = \sqrt{m\omega}$. The dynamics of a linear soliton in the harmonic trap have been introduced in Ref. [15]. The harmonic trap is capable of endowing a linear soliton with an inherent tendency of moving inward toward the trap center. Therefore, it is interesting to explore the competition between the harmonic trap and curvature-induced effective potential, as well as their impacts on the stability of the ring dark soliton. To date, it remains unclear which of the two will prevail over the other, or if they will end up evenly matched.

To investigate the underlying mechanism, we continue to employ a time-dependent simulation approach to study the competition process between these two motion trends. Analogous to approach used in the uniform case, we generate instantaneous ring dark solitons at four different initial locations. The results are shown in Fig. 3. From panel (a) to panel (d), instantaneous ring dark soliton is initially located at $r_0 k_F = 5.5, 9.0, 10.0$ and 12.2 , respectively. During the progress of time evolution, the ring soliton in panel (a) moves outwards, which is similar to the uniform case and means that the curvature-induced effective potential dominates over the effect from the harmonic trap. The ring soliton exhibits a significantly large oscillation amplitude. However, when r_0 is more and more far away from the center, for example $r_0 k_F = 9.0$ in panel (b), the ring soliton displays a narrow oscillation amplitude, although it still moves outwards initially. Something interesting is shown in panel (c), in which $r_0 k_F = 10.0$, it seems that the ring soliton is trying to be static at this position and shows an almost unobservable oscillation. Across this critical position, for instance $r_0 k_F = 12.2$ in panel (d), inversely the ring soliton initially moves inwards and again takes on an obvious oscillation amplitude. All these panels confirm that the outcome of the competition between the harmonic trap and the curvature-induced potential

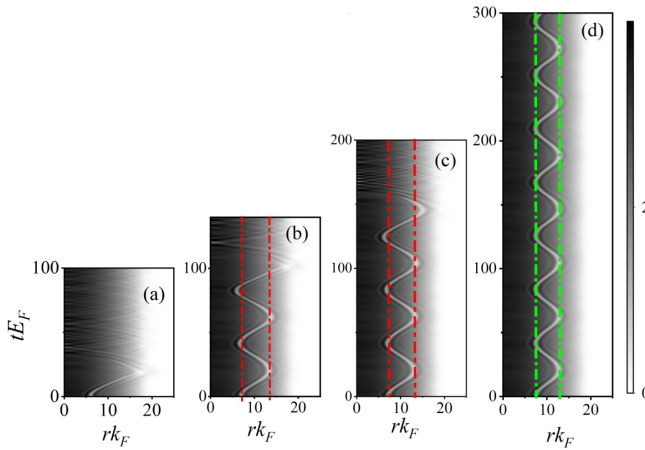


Figure 6. The time-evolution of ring solitons whose initial positions r_0 locate on the left-hand side of the stable location $r_s k_F = 10.1$. Their initial positions are respectively (a) $r_0 k_F = 6.0$, (b) $r_0 k_F = 7.0$, (c) $r_0 k_F = 7.2$ and (d) $r_0 k_F = 7.6$. The binding energy $E_b = 0.5E_F$.

is location-dependent. Notably, there exists a critical location at which the contributions of the aforementioned two factors are balanced with each other. This makes the ring dark soliton become a stable state at this equilibrium position ($r_s k_F \approx 10.0$).

To understand the underlying physical reason of generating stable ring soliton at r_s here, it is better to calculate the free energy of the instantaneous ring dark soliton. As shown in panel (b) of Fig. 4, the free energy takes on a local maximum around $r_s k_F = 10.1$, which is marked by a dotted arrow. This location is almost the same one in panel (c) of Fig. 3. Usually, a stable state of a many-body system should appear at the local (or global) minimum of free energy. In fact, this is true for the conventional wave of particles with positive mass. However, it is opposite for the soliton with negative mass. Thus, physically it can be understood why the stable soliton locates where free energy reaches maximum. Similar work on free energy of uniform ring dark soliton has also been done in panel (a), which shows a monotonously linear behavior without any local maximum or minimum. This also helps to explain why there is no stable ring dark soliton state in the uniform system. Here we use the outcome of the competition between the harmonic trap and curvature-induced effective potential to study the stable mechanism of the ring soliton. In fact, this strategy is universal and can be extended to various other complex systems characterized by the presence of ring dark solitons, including the imbalanced Fermi superfluid in Ref. [12].

We also numerically calculate the equilibrium location r_s at different binding energies E_b . As shown in Fig. 5, we can always obtain an equilibrium location r_s , whose value decreases with E_b and finally appears to be a constant value.

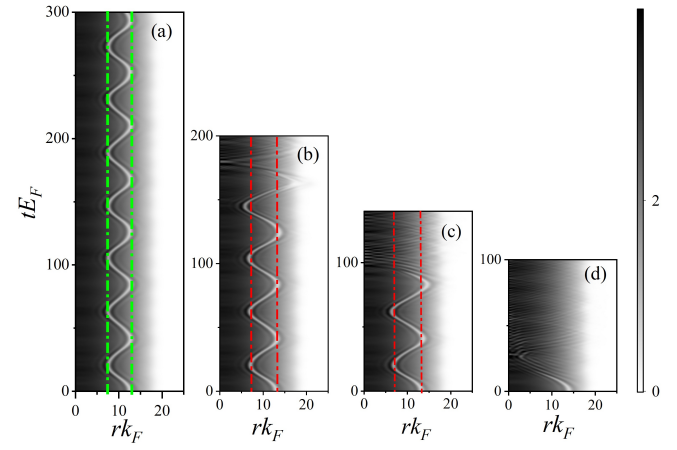


Figure 7. The time-evolution of ring solitons whose initial positions r_0 locate on the right-hand side of the stable location $r_s k_F = 10.1$. Their initial positions are respectively (a) $r_0 k_F = 12.6$, (b) $r_0 k_F = 13.0$, (c) $r_0 k_F = 13.2$ and (d) $r_0 k_F = 14.0$. The binding energy $E_b = 0.5E_F$.

C. Decay of ring solitons

Next it is natural to investigate what will happen when the ring dark soliton is not exactly located at equilibrium position r_s . It will be trivial if some dissipation immediately happens to ring soliton when its location is just slightly deviated from r_s , and make ring soliton decay. To check this, we carry out several time evolutions of ring soliton at different initial locations. As shown in Fig. 6, we prepare four zero-velocity ring solitons in different initial locations, namely $r_0 k_F = 6.0, 7.0, 7.2$ and 7.6 . To our surprise, we find different kind of dynamical oscillation behaviors of ring solitons. In panel (a), the initial radius r_0 of ring solitons is almost the order of its healing length displayed by the Friedel oscillation. The ring soliton quickly decays into sound wave ripples in a short time. The dynamical behaviors of panel (b) and (c) are different from the case in panel (a), we firstly watch a few periodic oscillations of ring solitons around equilibrium position r_s . The oscillation period is around $40/E_F$, whose value is determined by some inner parameters of the system [15]. It seems that there is a dissipation phenomenon occur to ring solitons, which gradually increases their oscillation amplitude. This phenomenon could be clearly observed by some red dot-dashed vertical lines, which initially marks the location with the maximum oscillation amplitude. Finally the ring soliton of panel (b) totally decayed into sound ripples in its third oscillation period, while the one in panel (c) in its fourth period due to its relatively bigger initial position r_0 (or closer to r_s). Different from other panels, the ring soliton in panel (d) experiences a longer oscillation time with a constant oscillation amplitude (marked by green dot-dashed lines). We carry out simulation to a long time ($tEF = 300$), whose value is almost twice of that in panel (c), while its

r_0 is just slightly bigger than that in panel (c). We can not see any obvious variation of its oscillation amplitude, and no sound ripples are generated. This means that a non-zero oscillation radius is existent, in which there is no dissipation occur to ring soliton during its periodic oscillation. It is interesting to investigate the physical reason behind these different dynamical phenomena.

It is obvious that the existence of ring solitons requires some space to present a non-zero radius. We find that these different dynamical behaviors can be explained by the competition between ring soliton's Friedel oscillation and its periodic oscillation around r_s . This competition is strong when r_0 comes into the effective regime of Friedel oscillation, brings energy dissipation to the periodic oscillation of ring soliton, and increases the maximum velocity of ring soliton (or oscillation amplitude). Once the maximum velocity reaches a critical velocity, determined by the minimum value between sound velocity and pair-breaking velocity, the ring soliton will totally decay into sound ripples [16]. This competition is absent in the periodic oscillation of linear solitons due to their straight-line geometry [15]. Once the radius is larger than the healing length of soliton's Friedel oscillation, this competition becomes weaker and weaker, and finally disappears after a sufficiently large radius, in which the ring soliton can always experience a periodic oscillation without any dissipation, just like the one in panel (d). Recently we notice that a similar dynamical behavior also happens in the ring soliton of spin-1 BEC system[26].

Different from the case in Fig. 6, all initial locations r_0 of ring solitons in Fig. 7 are on the right-hand side of equilibrium position r_s . Although all their initial radii r_0 are much bigger than the healing length of Friedel oscillation, this does not mean that their oscillation behaviors are always the one without dissipation. In fact, the periodic oscillation of ring soliton makes it possible to move to the left-hand side of r_s , and possibly induces the competition between Friedel oscillation and periodic oscillation of ring solitons. Thus similar dynamical oscillations of ring solitons can also be investigated, which are shown in four panels of Fig. 7. These dynamical behaviors share the same explanation discussed above. Compared with Fig. 6 and Fig. 7, it is easy to find similar dynamical behavior between left and right-hand side for a similar oscillation amplitude around r_s .

D. Ideal trap of ring dark soliton

Naturally, an intriguing question emerges: Does there exist an ideal trap capable of stabilizing a ring dark soliton at any position within the external trap? If such a trap exists, what geometric shape should it adopt? From all discussions above, it is sure that the curvature-induced effective potential can not be well balanced by the harmonic trap except the location r_s . In fact, some key factors may be implied by the free energy in Fig. 4. A linear dependence behavior is shown in the panel (a) of

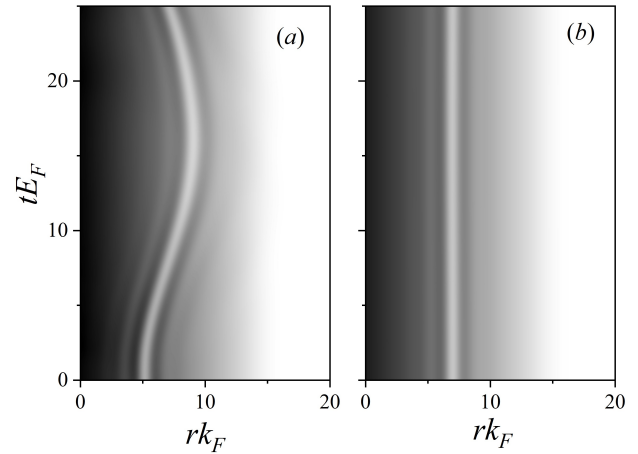


Figure 8. The evolution of ring solitons in a linear trap with different initial location, namely (a) $r_0 k_F = 5$ and (b) $r_0 k_F = 7$. The linear trap satisfies $V(\mathbf{r}) = 0.35|\mathbf{r}|$.

Fig. 4. It is easy to remind us to consider a linear external potential, namely $V(\mathbf{r}) \propto |\mathbf{r}|$. We have tried many sets of parameters in this kind of linear trap, and their simulations show similar results. The result of one of them is shown in Fig. 8, and demonstrates that the ring soliton can only be static at around $r_0 k_F = 7$, but not at other locations. This linear trap fails to generate a stable ring dark soliton anywhere. The investigation of an ideal structure of trap requires the analytical derivation of the expression of curvature-induced effective potential, which is not available currently.

IV. CONCLUSIONS

We theoretically investigate the stable mechanism of the ring soliton in a two-dimensional Fermi superfluid. By solving both static and time-dependent Bogoliubov-de Gennes equations, we find that the competition between external harmonic trap and curvature-induced potential play a key role of building a stable ring dark soliton. In the uniform case, the curvature-induced effective potential always drives the ring soliton away from their initial location and move outwards to the edge, which means there is no stable ring soliton solution in the uniform system. The introduction of a harmonic trap helps balance the curvature-induced effective potential, and makes the ring dark soliton be stable at an equilibrium location r_s , in which the free energy of the ring dark soliton just arrives at the maximum value. During the periodic oscillation of ring soliton around r_s , we find another competition between soliton's Friedel oscillation and periodic oscillation. This competition is strong once the minimum radius of the ring soliton is the order of healing length of Friedel oscillation. A dissipation effect occurs to ring soliton to increase its oscillation amplitude, and finally makes ring soliton decay into sound rip-

plexes. Once the ring soliton moves sufficiently far from the regime of Friedel oscillations, its periodic oscillations consistently exhibit a fixed amplitude and can persist indefinitely. Our research paves the way for us to understand the stable mechanism of a ring dark soliton in other different systems in the future.

V. ACKNOWLEDGMENTS

The authors acknowledge fruitful discussions with Xiaojian Yu and Xiaofei Zhang. This research is supported by the National Natural Science Foundation of China under Grants No. U23A2073 (P.Z.) and No. 12374250 (S.-G.P.), the National Key R&D Program under Grant No. 2022YFA1404102 (S.-G.P.), and Innovation Program for Quantum Science and Technology under Grant No. 2023ZD0300401 (S.-G.P.).

[1] P. G. Drazin and R. S. Johnson, *Solitons: An Introduction* (Cambridge University Press, Cambridge, England, 2002).

[2] P. G. Kevrekidis, D. J. Frantzeskakis, and R. Carretero-González, *Emergent Nonlinear Phenomena in Bose-Einstein Condensates, Theory and Experiment* (Springer, New York, 2007).

[3] J. Denschlag, J. E. Simsarian, D. L. Feder, C. W. Clark, L. A. Collins, J. Cubizolles, L. Deng, E. W. Hagley, K. Helmerson, W. P. Reinhardt, S. L. Rolston, B. I. Schneider, and W. D. Phillips, *Generating Solitons by Phase Engineering of a Bose-Einstein Condensate*, *Science* **287**, 97 (2000).

[4] S. Burger, K. Bongs, S. Dettmer, W. Ertmer, K. Sengstock, A. Sanpera, G. V. Shlyapnikov, and M. Lewenstein, *Dark Solitons in Bose-Einstein Condensates*, *Phys. Rev. Lett.* **83**, 5198 (1999).

[5] B. P. Anderson, P. C. Haljan, C. A. Regal, D. L. Feder, L. A. Collins, C. W. Clark, and E. A. Cornell, *Watching Dark Solitons Decay into Vortex Rings in a Bose-Einstein Condensate*, *Phys. Rev. Lett.* **86**, 2926 (2001).

[6] H. Sakaguchi and B. A. Malomed, *Dynamics of positive- and negative-mass solitons in optical lattices and inverted traps*, *J. Phys. B* **37**, 1443 (2004).

[7] C. Becker, S. Stellmer, P. Soltan-Panahi, S. Dörscher, M. Baumert, E.-M. Richter, J. Kronjäger, K. Bongs, and K. Sengstock, *Oscillations and interactions of dark and dark-bright solitons in Bose-Einstein condensates*, *Nat. Phys.* **4**, 496 (2008).

[8] G. Theocharis, D. J. Frantzeskakis, P. G. Kevrekidis, B. A. Malomed, and Yuri S. Kivshar, *Ring Dark Solitons and Vortex Necklaces in Bose-Einstein Condensates*, *Phys. Rev. Lett.* **90**, 120403 (2003).

[9] T. Yefsah, A. T. Sommer, M. J.H. Ku, L. W. Cheuk, W. Ji, W. S. Bakr, and M. W. Zwierlein, *Heavy solitons in a fermionic superfluid*, *Nature (London)* **499**, 426 (2013).

[10] W. Wang, P. G. Kevrekidis, and E. Babaev, *Ring dark solitons in three-dimensional Bose-Einstein condensates*, *Phys. Rev. A* **100**, 053621 (2019).

[11] W. Wang, T. Kolokolnikov, D. J. Frantzeskakis, R. Carretero-González, and P. G. Kevrekidis, *Pairwise interactions of ring dark solitons with vortices and other rings: Stationary states, stability features, and nonlinear dynamics*, *Phys. Rev. A* **104**, 023314 (2021).

[12] M. Barkman, A. Samoilenska, T. Winyard, and E. Babaev, *Ring solitons and soliton sacks in imbalanced fermionic systems*, *Phys. Rev. Research* **2**, 043282 (2020).

[13] M. Antezza, F. Dalfovo, L. P. Pitaevskii, and S. Stringari, *Dark solitons in a superfluid Fermi gas*, *Phys. Rev. A* **76**, 043610 (2007).

[14] R. Liao and J. Brand, *Traveling dark solitons in superfluid Fermi gases*, *Phys. Rev. A* **83**, 041604(R) (2011).

[15] R. G. Scott, F. Dalfovo, L. P. Pitaevskii, and S. Stringari, *Dynamics of Dark Solitons in a Trapped Superfluid Fermi Gas*, *Phys. Rev. Lett.* **106**, 185301 (2011).

[16] R. G. Scott, F. Dalfovo, L. P. Pitaevskii, S. Stringari, O. Fialko, R. Liao, and J. Brand, *The decay and collisions of dark solitons in superfluid Fermi gases*, *New J. Phys.* **14**, 023044 (2012).

[17] A. Cetoli, J. Brand, R. G. Scott, F. Dalfovo, and L. P. Pitaevskii, *Snake instability of dark solitons in fermionic superfluids A*, *Phys. Rev. A* **88**, 043639 (2013).

[18] K. Sacha, and D. Delande, *Proper phase imprinting method for a dark soliton excitation in a superfluid Fermi mixture*, *Phys. Rev. A* **90**, 021604(R) (2014).

[19] L. Kong, G. Fan, S.-G. Peng, X.-L. Chen, H. Zhao, and P. Zou, *Dynamical generation of solitons in one-dimensional Fermi superfluids with and without spin-orbit coupling*, *Phys. Rev. A* **103**, 063318 (2021).

[20] Y. Xu, L. Mao, B. Wu, and C. Zhang, *Dark Solitons with Majorana Fermions in Spin-Orbit-Coupled Fermi Gases*, *Phys. Rev. Lett.* **113**, 130404 (2014).

[21] X.-J. Liu, *Soliton-induced Majorana fermions in a one-dimensional atomic topological superfluid*, *Phys. Rev. A* **91**, 023610 (2015).

[22] A. M. Mateo, and X. Yu, *Two types of dark solitons in a spin-orbit-coupled Fermi gas*, *Phys. Rev. A* **105**, L021301 (2022).

[23] P. Zou, J. Brand, X.-J. Liu, and H. Hu, *Traveling Majorana Solitons in a Low-Dimensional Spin-Orbit-Coupled Fermi Superfluid*, *Phys. Rev. Lett.* **117**, 225302 (2016).

[24] H. Guo, Y.-J. Wang, L.-X. Wang, X.-F. Zhang, *Dynamics of ring dark solitons in Bose-Einstein condensates*, *Acta Phys. Sin.*, **2020**, **69**(1): 010302.

[25] H. Tamura, C.-A. Chen, and C.-L. Hung, *Observation of Self-Patterned Defect Formation in Atomic Superfluids from Ring Dark Solitons to Vortex Dipole Necklaces*, *Phys. Rev. X* **13**, 031029 (2023).

[26] X. Yu, *Oscillating ring ferrodark solitons with breathing nematic core in a homogeneous spinor superfluid*, *arXiv: 2509.13874v2*.